Update on the NCAR Thunderstorm Nowcast System

Cynthia Mueller, Tom Saxen, Rita Roberts and Jim Wilson
National Center for Atmospheric Research[1]

Introduction

This paper provides an update on NCAR Auto-Nowcast System (AN), a software system that produces time and space specific 0-1 hr nowcasts[2] of convective storm location and intensity. AN combines observations, a numerical boundary-layer model and it's adjoint (Variational Doppler Radar Analysis System, VDRAS, Sun and Crook 2001), forecaster input, and feature detection algorithms to provide routine nowcasts of thunderstorm position. AN was developed by the National Center for Atmospheric Research with prime funding from the Federal Aviation Administration[3].

A primary and unique component of AN is its ability to identify and characterize boundary-layer convergence lines. Feature detection algorithms and VDRAS are used to monitor and nowcast boundary-layer structure. The importance of the boundary-layer in thunderstorm development was first shown by the Thunderstorm Project (Byers and Braham 1949). Purdom (1973,1976, 1982) indicated the importance of monitoring cloud lines with satellite data to nowcast storms. Wilson and Carbone (1984) suggested the utility of radar-detected clear-air "boundaries" for use in thunderstorm nowcasting. Wilson and Mueller (1993, hereafter WM93) provided conceptual models for using boundaries to nowcast thunderstorm evolution. These conceptual models form the basis for many of the nowcasting procedures. In this paper, a case study illustrates the importance of various predictors, listed in Table 1, to the nowcast of convective storms at 30 and 60-min periods.

AN System Methodology

Operational data sets used in the system include full-resolution radar (generally WSR-88D), satellite, surface stations (including special mesonets), lightning, profilers, numerical model, and radiosondes. These data are input into analysis algorithms to calculate predictor fields. Analysis algorithms include data quality control routines, feature detection algorithms, and VDRAS to obtain thunderstorm predictor fields. In some cases, it is beneficial for a forecaster to interact with AN by manually inputting the position of boundaries. Because the algorithm learns from the forecaster, this does not have to be done routinely. The predictor fields are combined using a fuzzy logic. The fuzzy logic approach uses membership functions to map the predictor fields to the likelihood of storms (likelihood fields). The dimensionless likelihood fields are meant to represent quantitatively the relationship between the predictor fields (e.g. low-level convergence) and the existence of a convective storm at each point of a horizontal grid. The likelihood fields are weighted and summed to produce a combined likelihood field. The combined likelihood field is filtered and thresholded to generate the nowcast areas of convective activity.

Examples of Initiation, Growth and Dissipation Nowcasts

This Section presents examples of initiation, growth, and dissipation nowcasts using a case from 5 July 2001 in the Denver, Colorado area. On this day, synoptic scale forcing over Colorado was weak. The steering level winds were approximately 5 m s-1 from the southeast. Surface dew points were ~10^{o}C, typical for a storm day in Colorado. A storm formed, grew and dissipated within the AN domain. During the storm, Denver International Airport's ground operations were shut down for over an hour while the storm

Predictors (units)	Initiation		Growth		Dissipation	
	30	60	30	60	30	60
1. Extrapolated reflectivity (dBZ)			*	+	+	+
2. Extrapolated reflectivity with stratiform regions removed (dBZ)			-	-		
3. Storm Area (km2)			-	-		
4. Negative and positive growth rates (km2/hr)			*	+	*	*
5. Precipitation Accumulation (mm)						
6. Boundary location and speed (m/s)	-	-	-	-	*	*
7. Boundary collision and Boundary storm collision	+	*	*	*		
8. Boundary relative steering flow (m/s)	*	+	+	+		
9. Boundary relative low-level shear (m/s)						
10. MaxW (m/s)	*	*	*	*		
11. Radar Cumulus (dBZ)	*		+			

Table 1 List of predictors used in the NIWOT along with their subjective contribution to the July 5, 2001 forecast of initiation, growth, and dissipation. A "" indicates it was a major factor, "+" indicates a significant factor and " –" a contributing factor.*

1. The National Center for Atmospheric Research is partially funded by the National Science Foundation. This research is partially sponsored by the National Science Foundation through an Interagency Agreement in response to requirements and funding by the Federal Aviation Administration's Aviation Weather Research Program.

2. The word nowcast is used in this paper to emphasize that the nowcasts are time and space specific for periods less than a few hours. The nowcasts may include initiation, growth and dissipation of storms

3. FAA support is presently through the Aviation Weather Research Program (AWRP) as part of the Convective Weather Product Development Team (Wolfson et. al. 1997). Additional support has been received from the Army Test and Evaluation Command (ATEC), National Science Foundation (NSF) portion of the U.S. Weather Research Program and the Radar Operations Center of the National Weather Service.

produced a good deal of lightning and hail.

The 30-min AN nowcasts are shown in Fig 1a, c and e by the white lines with the corresponding verification data shown in Fig 1b, d, and f. The nowcast panels are at 40-min intervals. The nowcasts are for the initiation of storms associated with a boundary collision (Figs 1a and b), continued storm growth.(Figs 1c and d) and dissipation as the boundary moves away from the storm (Figs 1e and f). In general, AN nowcasts for both 30 and 60 min are quite good. Figure 2, shows probability of detection (POD) and false alarm rate (FAR) for the period. Four nowcast techniques were evaluated; (1) persistence, (2) extrapolation, (3) AN with automated boundaries and (4) AN with human boundaries. Table 1 lists the relative contributions of AN predictor fields for 30-min and 60-min initiation, growth, and dissipation portions of the nowcasts. The table shows a subjective evaluation of which predictors were the most important to the nowcasts.

The primary contributors to the 30-min initiation nowcast are the Radar Cumulus and Boundary Relative Steering Flow. The Radar Cumulus shows the presence of convective echoes between 0-55 dBZ in the height range 3-6 km. The Boundary Relative Steering Flow show regions where the vector difference between the steering level winds and the boundary motion is small, thus allowing an updraft into a developing storm to be maintained. At 30-min, these two fields are sufficient to produce a nowcast in regions of overlap. At 60-min these criteria are not sufficient. For longer period nowcasts, accurate characterization of the boundary-layer forcing becomes crucial to the nowcast. In this case, the collision and strength of the boundary convergence are the most important factors in the 60-min nowcast.

The nowcasts for continued growth at both 30 and 60 min were based heavily on a strong positive vertical motion determined from VDRAS winds, storm-boundary collision, and positive storm area growth. The 30-min nowcast also uses Radar Cumulus. For the 30-min nowcast, the extrapolated storm positions, Radar Cumulus and storm area trend play a much larger role then in the 60-min nowcast. The 60-min nowcast is more dependent on the environmental conditions associated with the boundaries (e.g. MaxW) and boundary-storm collision.

Finally, during the dissipation stage, both the 30-min and 60-min nowcasts were based on the absence of a boundary and negative growth rates.

The nowcast statistics, Fig 2, indicate that AN has significant skill over either persistence or extrapolation at both 30 and 60-min nowcasts. The 30-min AN forecasts with human boundaries and automated boundaries show similar skill throughout the forecast period. Review of the two forecast shows that AN using human boundaries covered slightly larger areas than the automated version, but the nowcast locations were basically the same. However, the automated and human boundaries were not the same. The automated system only captured the boundary coming from the north and the motion vector was too fast. However, even with the poor detection by the automated system, both human and automated systems had boundary relative steering level speed field that was favorable for initiation and that overlapped with a Radar Cumulus field. Thus both automated and human systems met the minimum requirements for an initiation nowcast and because the Radar Cu field was the same for both systems, the nowcasts were similar. However, in the case of the 60-min nowcasts, the verification statistics (Fig. 2 b, and d) indicate that the human-boundary nowcasts captured the initiation 30 min prior to the automated system. For the 60-min nowcasts the boundary characteristics were the primary contributors and in this case boundary collision was the most important field. The automated system was unable to detect either of the southern boundaries and therefore missed the collision and did not produce a timely initiation nowcast.

Short-term nowcasts of less than 30 min depend primarily on accurate detection and extrapolation of the cumulus field either as determined on satellite or radar, and storm trends in association with a boundary. As the nowcast period increases, accurate knowledge of the boundary-layer structure and stability become more important. In all cases, accurate extrapolations of the various fields are required and are often difficult to obtain; thus decreasing the potential specificity of the nowcast.

Conclusion

AN is used to its best advantage in the prediction of boundary-layer forced storms, it performs well in conditions of both weak (White Sands) and strong (Sterling) synoptic forcing. Boundary detection and characterization are crucial to nowcasts of storm initiation, growth, and dissipation. Automated boundary detection algorithms tend to provide adequate skill for a 30-min storm forecast because the nowcasts are primarily dependent on radar and satellite observations of the current storms and trends in their size. Although accurate 30-min nowcasts of storms are significantly affected by boundary detection, the determination of boundary characteristics is not so crucial for 30-min nowcasts as compared to the 60-min nowcasts. At longer time periods, current storms and trends are less important to the nowcasts because the lifecycle of convective elements is generally less than an hour (Battan 1953; Foote and Mohr 1979; Henry 1993). Accurately nowcasting boundary-layer forcing, shear, and instability becomes more important. Thus, boundary detection and extrapolation need to be accurate. With today's technology, consistently accurate boundary detections and extrapolations require a forecaster's input. The capability for real-time human input to help guide the automated system is currently incorporated into AN. Additional effort is required to ensure the temporal continuity of the boundaries.

Correctly extrapolating the various predictor fields, which all tend to move with different motion vectors, is another difficult problem that tends to become more problematic with longer nowcast intervals. Extrapolating the position of objects that have a steady motion for at least three time periods is generally good. However in many cases motions are not steady or there is not a history. Important situations that are often incorrectly predicted include: clouds not moving with the steering level winds and instead remaining attached to the boundary thus moving with the boundary motion; severe storms becoming right movers or developing a bow; boundaries stalling or accelerating; and initial storm motions being incorrectly based on steering level winds when the storm is in fact tied to a forcing feature such as terrain or boundaries.

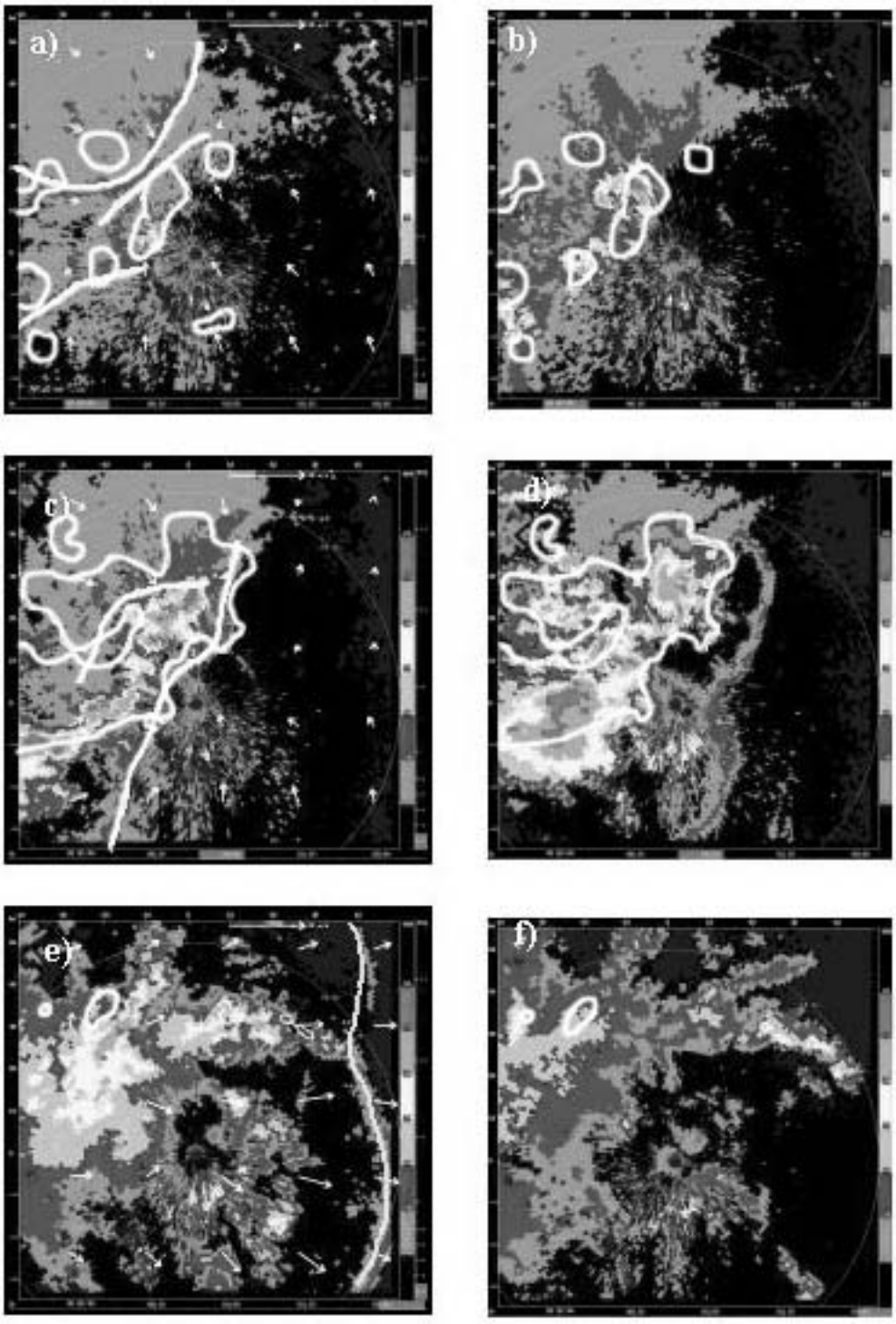

Figure 1. Nowcasts (frames a, c and e) and verification (frames b, d and f) for 5July 2001 Denver CO area. Frames a, c and e are at ~40 min intervals. The white vectors indicate VDRAS low-level winds and the thick white lines indicate human-entered boundaries. The white contours are 30-min nowcasts. In frames a, c and e the nowcast issued at the time of radar PPI's are shown. The radar echoes that existed at the corresponding prediction times are shown in frames b, d and f.

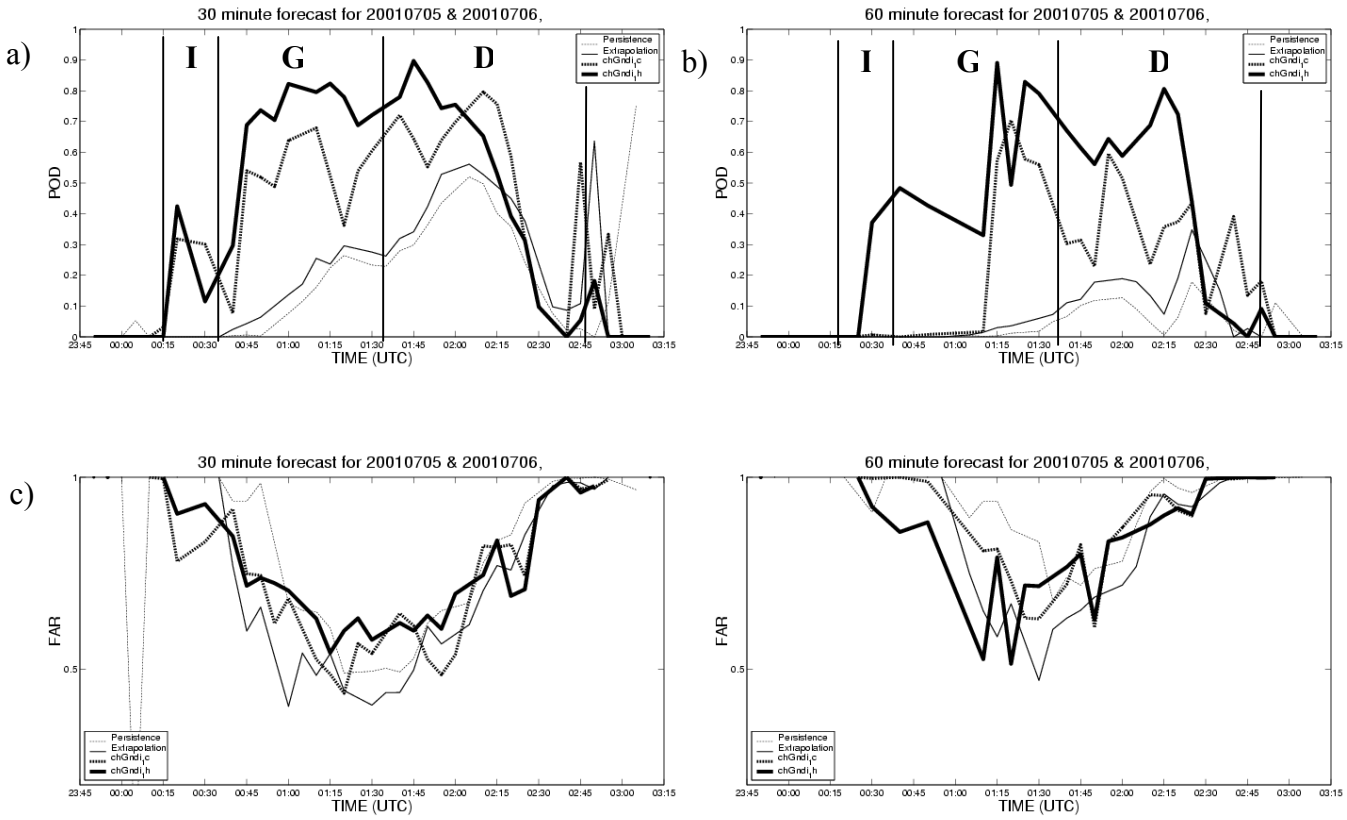

Figure 2. Validation statistics for 30 and 60 min forecasts for 5 July 2001 are shown. Frames a and b are POD scores for 30 and 60-min nowcasts respectively, and frames c and d FAR for 30 and 6- min nowcasts respectively. The broken light gray, solid light gray, broken medium gray, and solid black lines show nowcasts for persistence, extrapolation, Nowcaster with automated boundaries and Nowcaster with human-entered boundaries. Initiation (I), growth (G), and dissipation (D) phases are indicated.

Stability issues also become more important as the nowcast period and domain increase. Currently AN uses clouds as a proxy for stability since there is no operational direct means for obtaining high resolution stability information. This tends to work well for short-periods (0-30 min), but longer-period nowcasts require more direct measurements and nowcasts of stability. Efforts are on-going to incorporate stability parameters from meso-scale numerical models into AN. New water vapor observing technologies are also being closely followed. Presently the convergence and vertical motion associated with boundaries is based on retrievals from VDRAS. Efforts are underway to enhance VDRAS to forecast boundary layer winds for periods of 1-2 hr.

References:

Byers, H.R., and R.R. Braham, Jr., 1949: *The Thunderstorm.* U.S. Govt. Printing Off., Washington, D.C., 187 pp.

Mueller, C.K., T. Saxen, R. Roberts, and J.W. Wilson, 2000: Evaluation of the NCAR Thunderstorm Auto-AN. Preprints, *9th Conf. On Aviation Meteorology*, Orlando, Florida, Pp. 40-45.

Purdom J.F.W., 1973: Satellite imagery and the mesoscale convective forecast problem, Preprints, *8th Conference on Severe Local Storms*, Denver, Amer. Meteor. Soc. 244-251.

Purdom, J. F. W., 1976: Some uses of high resolution GOES imagery in the mesoscale forecasting of convection and its behavior. *Mon. Wea Rev.*, **104**, 1474-1483.

Purdom, J.F.W., 1982: Subjective interpretations of geostationary satellite data for nowcasting. *Nowcasting*, K. Browning (Ed.), Academic Press, London, 149-166.

Roberts, R, T. Saxen, C. Mueller, J. Wilson, A. Crook, J. Sun and S. Henry, 1999: Operational application and use of NCAR's thunderstorm nowcasting system. Preprints, 15th International Conf. on Interactive Information and Processing Systems (IIPS) Eighth Conf., Amer. Meteor. Soc., Dallas TX, 158-161.

Sun, J. And N.A. Crook, 2001: Real-time low-level wind and temperature analysis using single WSR-88D data. *Wea. Forecasting,* **16**, 117-132.

Wilson, J.W., and R. Carbone, 1984: Nowcasting with Doppler radar: The forecaster-computer relationship. *Nowcasting II*, K. Browning (Ed.), European Space Agency, Paris, France, 177-186.

Wilson, J.W., N. A. Crook, C. K. Mueller, J. Sun and M. Dixon, 1998: Nowcasting Thunderstorms: A Status Report. *Bull. Amer. Meteor. Soc.*, **79**, 2079-2099.

Wilson, J. W., and C. K. Mueller, 1993: Nowcasts of thunderstorm initiation and evolution. *Wea. Forecasting.*, **8**, 113-131.